Synthesis, Characterization, and Magnetic Property of a Novel Dimer-of-Di(μ-oxo)dimanganese-Dimers with Two Coordinated Water Molecules in (III,IV,III,IV) Oxidation State

Hisano KAWASAKI, Masami KUSUNOKI,*,† Yoshihito HAYASHI, Masatatsu SUZUKI,* Kazutoshi MUNEZAWA, Machiko SUENAGA, Hitoshi SENDA,†† and Akira UEHARA*

Department of Chemistry, Faculty of Science, Kanazawa University, Kanazawa 920-11
† Department of Physics, School of Science and Technology, Meiji University, Kawasaki 214
†† Laboratory of Chemistry, Faculty of Liberal Arts, Kanazawa University, Kanazawa 920-11

(Received December 9, 1993)

A dimer-of-di(μ-oxo)manganese(III)manganese(IV)-dimers with two coordinated water molecules, [{Mn_2(tmdp)$(O)_2(H_2O)$}$_2$]$(CF_3SO_3)_4\cdot 6H_2O$ (**1**), was prepared, where Htmdp is 1,5-bis[bis(2-pyridylmethyl)-amino]-3-pentanol. Crystal structure of **1** was determined by X-ray structure analysis. **1** crystallizes in triclinic space group, $P\bar{1}$ with $a=16.543(1)$, $b=19.097(2)$, $c=13.393(1)$ Å, $\alpha=94.450(7)°$, $\beta=90.698(6)°$, $\gamma=84.997(7)°$, $V=4202.4(6)$ Å^3, and $Z=2$. The complex cation consists of two di(μ-oxo)manganese(III)manganese(IV) dimers which are linked by two tmdps and hydrogen bonding network between two coordinated water molecules and two alkoxo groups to form a dimer-of-dimers with a bilayered structure with dimer-dimer separation of 5.9 Å. The Mn–Mn separations are 2.644(2)—2.651(2) Å. Magnetism of **1** was well interpreted in terms of the model based on two kinds of the exchange interactions between Mn(III) and Mn(IV); the intradimer interaction ($J_1=-145$ cm^{-1}) through di(μ-oxo) bridges and the interdimer interaction ($J_2\cong -0.2$ cm^{-1}) through hydrogen bonding network. The interdimer exchange interaction (J_2) results in a triplet ground state. The ESR spectrum of a frozen solution sample of **1** showed a relatively intense "$\Delta M_s=2$" signal centered at $g=4.5$, which is only 7.6 times weaker than a much broader "$\Delta M_s=1$" signal at $g=2.0$. The best computer simulation revealed near rhombic zero-field splittings with $|D|\cong 0.07$ cm^{-1} and $|E|\cong 0.023$ cm^{-1}, and Mn-hyperfine broadening, which are appropriate for the triplet ground state of such a tetrameric dimer-of-di(μ-oxo)manganese(III)manganese(IV)-dimers with 5.9 Å separation. The observed zero-field splittings could be interpreted in terms of an incomplete quenching of the crystal field effect of each Mn(III) ion in the triplet ground state mixed with the excited-state spin configurations through the J_2 interactions. Cyclic voltammogram exhibited a quasi reversible wave ($E_{1/2}=0.98$ V vs. SCE) and an irreversible oxidation wave at 1.10 V vs. SCE in acetonitrile. Constant potential electrolysis at 1.00 V vs. SCE indicated that the quasi reversible wave is a one-electron transfer process and corresponds to Mn_4(III, IV, IV, IV)/Mn_4(III, IV, III, IV) redox couple. A one-electron oxidized species which was generated electrochemically showed a so called sixteen hyperfine pattern at $g=2.0$, supporting the presence of di(μ-oxo)manganese(III)manganese(IV) and di(μ-oxo)dimanganese(IV) species in the tetramer. Constant potential electrolysis at 1.20 V vs. SCE resulted in a decomposition of the complex.

The oxygen-evolving center (OEC) in photosystem II (PS II) in green plants and algae has been shown to contain a tetranuclear manganese center which catalytically oxidizes two water molecules to molecular oxygen.[1] Although the nature of the manganese center and the reaction mechanism of water oxidation are ambiguous, the presence of di(μ-oxo)dimanganese unit in the tetramer has been proposed in the S_1 and S_2 states in Kok's S state scheme[2] by ESR, EXAFS, and XANES studies.[3] A variety of tetranuclear manganese complexes in various oxidation states[4] have been devised as structural and spectroscopic models for the S_n states in PS II.

For approaching the more precise models of OEC, it is important to devise polynuclear manganese complexes that contain two water molecules as a molecular oxygen source in coordination sphere and are four-electron oxidants having enough redox potentials for water oxidation. Such functional models, however, have not been reported so far.

In the previous studies, we found that the tripodal ligands tend to form di(μ-oxo)dimanganese core, because tripodal ligands can provide two vacant coordination sites in *cis*-position for formation of two oxo bridges. The heptadentate ligand tpdp (1,3-bis[bis(2-pyridylmethyl)amino]-2-propanolate) which has two tripodal parts forms three types of tetranuclear complexes, i.e. Mn(II)–Mn(III)–O–Mn(III)–Mn(II),[4f,4g] Mn(II)–Mn(III)$<^{O}_{O}>$Mn(IV)–Mn(II),[4h,4i] and (Mn(III)$<^{O}_{O}>$Mn(IV))$_2$.[4j] Since the present ligand tmdp also contains tripodal parts, it was expected that the ligand forms polynuclear complexes with di(μ-oxo)dimanganese core(s).

Dexheimer and Klein[5] have reported that the S_1 state of the OEC shows a broad parallel polarization signal at $g=4.8$, which has been simulated with an $S=1$ spin-Hamiltonian with $g=2$ and zero-field splitting parameters of $D=0.125$ cm^{-1} and $E=0.025$ cm^{-1}. Recently, Kirk et al.[6] reported that a complex [(Mn_2O_2)$_2$(tphpn)$_2$]$^{4+}$ which has a (III,IV,III,IV) oxidation state as well as that of the present complex has a triplet ground state and shows a similar parallel polarization ESR signal at $g\cong 6$. From the magnetism of the complex, the zero-field splitting constants are estimated to

be $D=1.8$ cm^{-1} and $E=-0.15$ cm^{-1}. They suggested that the pseudo-dipolar interaction between two di(μ-oxo)manganese(III)manganese(IV) dimers through alkoxo bridges is the dominant contribution for the observed zero-field splitting. In order to get further insight into the electronic structure of such tetranuclear manganese complexes, it is important to elucidate the origin of zero-field splitting.

In this study, we report the synthesis, structural characterization, and some physicochemical properties of a novel dimer-of-di(μ-oxo)manganese(III)manganese(IV)-dimers with two coordinated water molecules, $[\{Mn_2(tmdp)(O)_2(H_2O)\}_2](CF_3SO_3)_4\cdot 6H_2O$. The complex showed a broad "$\Delta M_s=1$" EPR signal at $g=2$ and a relatively strong "$\Delta M_s=2$" signal at $g=4.5$. The theoretical approach to elucidate the origin of zero-field splitting of this was also made.

Experimental

Materials. Htmdp was synthesized according to the literature.[7] The other chemicals are of reagent grade.

Preparation of Complexes. $[\{Mn_2(tmdp)(O)_2H_2O\}_2](CF_3SO_3)_4\cdot 6H_2O$(1): An ethanol solution (10 cm^3) of Htmdp (0.5 mmol) was mixed with an aqueous solution (5 cm^3) of $Mn(NO_3)_2\cdot 9H_2O$ (2 mmol). To the resulting mixture were successively added triethylamine (0.5 mmol) in 2.5 cm^3 of ethanol and CF_3SO_3Na (3 mmol) in 2 cm^3 of water. The reaction solution was gradually oxidized with air to give dark brown solution. The resulting solution was allowed to stand for several days to give dark green crystals; yield 50 mg. Found: C, 37.47; H, 4.06; N, 8.44%. Calcd for $Mn_4C_{62}H_{82}N_{12}F_{12}O_{26}S_4$: C, 37.47; H, 4.16; N, 8.46%.

$[\{Mn_2(tmdp)(O)_2H_2O\}_2](ClO_4)_4$ (1a): To a solution of $Mn(ClO_4)_2\cdot 6H_2O$ (1 mmol) in 5 cm^3 of water was added Htmdp (0.5 mmol) and triethylamine (0.5 mmol) in 12.5 cm^3 of ethanol. The reaction solution was gradually oxidized with air to give dark brown solution. The resulting solution was allowed to stand for several days to afford dark green crystals; yield 80 mg. Found: C, 40.61; H, 4.47; N, 9.69%. Calcd for $Mn_4C_{58}H_{70}N_{12}O_{24}Cl_4$: C, 40.12; H, 4.07; N, 9.69%.

Measurements. The electronic spectra were measured on a Hitachi U-3400 spectrophotometer. The infrared spectra were obtained by the KBr-disk method with a Horiba FT-200 spectrophotometer. The magnetic susceptibilities were measured with a SQUID susceptometer of QUANTUM DESIGN MPMS Model which was calibrated with Hg[Co(NCS)$_4$]. Diamagnetic correction was made by using Pascal's constant.[8] Cyclic voltammograms were obtained with a Hokuto Denko HA-301 Potentionstat/Galvanostat and a Hokuto Denko HB-104 Function Generator by using a three-electrode configuration, including a glassy carbon working electrode, a platimum-coil auxiliary electrode, and a saturated calomel electrode as a reference electrode. Acetonitrile was used as the solvent, and tetrabutylammonium perchlorate as a supporting electrolyte. Constant-potential electrolyses were performed with a Hokuto Denko HA-301 Potentionstat/Galvanostat by using a two compartmental H-type cell separated by a polypropylene film (JURAGUARD-2500), and the cell was equipped with a platinum gauze working electrode, a platinum plate auxiliary electrode, and a saturated caromel electrode. The integration of the current was carried out by integrating the area of the current vs. time curve. X-Band ESR spectra were measured on a JEOL JES-RE1X ESR spectrometer and a JEOL JES-FE2XG ESR spectrometer (X-band microwave unit, 100 kHz field modulation). The band frequency was calibrated with 1,1-diphenyl-2-picrylhydrazyl (DPPH, $g=2.0036$).

X-Ray Crystallography. Single Crystals suitable for X-ray study were obtained by recrystallization from acetonitrile–water mixture (1 : 1). A dark green prismatic crystal with dimensions of $0.3\times 0.3\times 0.4$ mm was used for X-ray crystal structure analysis. Data were collected on a Rigaku AFC-5R four circle automated diffractometer with graphite monochromated Mo $K\alpha$ radiation ($\lambda=0.71073$ Å) at room temperature. Unit cell parameters were determined by a least-squares fit to 25 reflections having $30.0°<\theta<40.0°$. Crystallographic data are summarized in Table 1. Three standard reflections were measured every 150 reflections, which show no systematic decay throughout data collection. The data were corrected for Lorentz and polarization effects and an empirical absorption correction (Ψ scans) was also applied (transmission factor ranges from 1.000 to 0.927). The structure was solved by direct method using the program SHELXS-86.[9] Full-matrix least-squares refinement and difference Fourier method (SHELX-76)[10] were used to locate all remaining non-hydrogen atoms. The atomic scattering factors and anomalous dispersion coefficients were taken from the literature.[11] Although the elemental analysis and the density measurement ($\rho=1.60$ g cm^{-3}) of the crystals suggested that the complex contains six lattice water molecules, only two lattice water molecules were found, which is probably due to serious disorder of the remaining

Table 1. Crystallographic Data for Complex **1**

Formula	$Mn_4C_{62}H_{82}N_{12}F_{12}O_{26}S_4$
FW	1987.36
Space group	$P\bar{1}$
a/Å	16.543(1)
b/Å	19.097(2)
c/Å	13.393(1)
α/deg	94.450(7)
β/deg	90.698(6)
γ/deg	84.997(7)
V/Å^3	4202.4(6)
Z	2
Crystal size/mm	$0.3\times 0.3\times 0.4$
ρ_{calcd}/g cm^{-1}	1.57
ρ_{obsd}/g cm^{-1}	1.60
λ(Mo $K\alpha$)/Å	0.71073
Scan method	ω–2θ
Scan speed/° min^{-1}	6
Max scan times	3
No. of data collected	16984
No. of data used	11335($\|F_o\|\geq 4.0\sigma\|F_o\|$)
Range/ deg	$3\leq 2\theta\leq 60$
T/°C	23
μ/cm^{-1}	8.45
R	0.092
R_w	0.117

Table 2. Fractional Atomic Coordinates of **1** with Their Standard Deviations in Parentheses [a)]

Atom	x	y	z	U_{eq}	Atom	x	y	z	U_{eq}
Mn1a	0.3462(1)	0.4164(1)	0.0665(1)	0.037(1)	C6b	0.0655(7)	0.1880(6)	0.4584(8)	0.052(6)
Mn2a	0.3690(1)	0.5372(1)	0.1689(1)	0.039(1)	C7b	0.1368(6)	0.0773(6)	0.1105(7)	0.053(6)
O1a	0.4207(1)	0.4477(3)	0.1516(5)	0.040(3)	C8b	0.2087(6)	0.1017(5)	0.1704(7)	0.046(6)
O2a	0.2900(4)	0.5004(3)	0.0900(5)	0.042(4)	C9b	0.2759(7)	0.1258(6)	0.1280(9)	0.058(7)
O3a	0.3967(4)	0.4390(3)	−0.0499(4)	0.042(4)	C10b	0.3400(7)	0.1439(7)	0.1913(10)	0.068(8)
O4a	0.4407(4)	0.5717(4)	0.0391(5)	0.049(4)	C11b	0.3340(7)	0.1386(6)	0.2932(9)	0.055(7)
N1a	0.2515(5)	0.3697(4)	−0.0115(6)	0.048(5)	C12b	0.2646(6)	0.1138(5)	0.3307(8)	0.048(6)
N2a	0.4041(5)	0.3175(4)	0.0365(6)	0.044(4)	C13b	0.2993(6)	−0.0570(6)	0.5387(8)	0.052(6)
N3a	0.2921(5)	0.3724(4)	0.1785(6)	0.045(5)	C14b	0.3295(7)	−0.0489(5)	0.2691(8)	0.054(6)
N4a	0.4491(5)	0.5817(4)	0.2816(6)	0.042(4)	C15b	0.4133(8)	−0.0462(7)	0.2594(11)	0.075(9)
N5a	0.3107(5)	0.5234(4)	0.3161(6)	0.046(5)	C16b	0.4628(8)	−0.0503(8)	0.3440(11)	0.076(9)
N6a	0.3243(5)	0.6416(4)	0.1694(6)	0.049(5)	C17b	0.4280(7)	−0.0546(7)	0.4366(10)	0.073(8)
C1a	0.2747(7)	0.2937(5)	−0.0416(9)	0.056(7)	C18b	0.3438(6)	−0.0551(6)	0.4414(8)	0.050(6)
C2a	0.3623(6)	0.2724(5)	−0.0231(7)	0.048(6)	C19b	0.2551(6)	−0.1737(5)	0.4954(8)	0.050(6)
C3a	0.4000(8)	0.2068(6)	−0.0589(9)	0.063(7)	C20b	0.1199(7)	−0.1912(6)	0.2764(9)	0.061(7)
C4a	0.4785(8)	0.1894(7)	−0.0324(10)	0.069(8)	C21b	0.1098(8)	−0.2616(7)	0.2651(11)	0.072(9)
C5a	0.5211(8)	0.2348(6)	0.0297(10)	0.064(8)	C22b	0.1468(8)	−0.3075(6)	0.3313(11)	0.073(9)
C6a	0.4824(6)	0.2997(6)	0.0636(8)	0.052(6)	C23b	0.1933(7)	−0.2792(6)	0.4101(10)	0.063(7)
C7a	0.1829(6)	0.3781(6)	0.0624(9)	0.059(7)	C24b	0.2004(6)	−0.2073(5)	0.4179(8)	0.045(6)
C8a	0.2148(7)	0.3576(5)	0.1600(8)	0.053(6)	C25b	−0.0038(6)	0.0516(6)	0.1289(7)	0.055(6)
C9a	0.1697(8)	0.3275(6)	0.2306(10)	0.071(8)	C26b	−0.0799(6)	0.0578(6)	0.1942(7)	0.054(6)
C10a	0.2063(9)	0.3105(7)	0.3200(11)	0.076(9)	C27b	−0.0676(6)	0.0167(5)	0.2860(6)	0.041(5)
C11a	0.2863(9)	0.3244(6)	0.3377(9)	0.072(8)	C28b	−0.1465(6)	0.0175(5)	0.3469(7)	0.043(5)
C12a	0.3300(7)	0.3558(5)	0.2655(8)	0.054(6)	C29b	0.1778(6)	−0.0927(5)	0.6166(7)	0.045(6)
C13a	0.4510(7)	0.5349(6)	0.3661(7)	0.051(6)	S1	0.6907(2)	0.0586(2)	0.0631(3)	0.066(2)
C14a	0.2324(7)	0.5103(5)	0.3298(9)	0.055(6)	S2	0.5777(3)	0.3271(2)	0.3785(3)	0.087(3)
C15a	0.2062(8)	0.4959(7)	0.4242(10)	0.070(8)	C31	0.6093(9)	0.0323(8)	0.1324(12)	0.083(10)
C16a	0.2618(9)	0.4955(8)	0.5019(10)	0.081(9)	C32	0.5496(11)	0.2416(9)	0.3481(15)	0.099(12)
C17a	0.3418(8)	0.5085(7)	0.4870(9)	0.071(8)	F1	0.5468(6)	0.0785(6)	0.1429(9)	0.136(9)
C18a	0.3641(6)	0.5216(5)	0.3915(7)	0.048(6)	F2	0.5850(7)	−0.0270(6)	0.0936(11)	0.166(11)
C19a	0.4092(7)	0.6545(5)	0.3160(8)	0.051(6)	F3	0.6320(9)	0.0211(9)	0.2225(9)	0.189(13)
C20a	0.2766(8)	0.6654(6)	0.0945(9)	0.066(8)	F4	0.4862(6)	0.2384(5)	0.2890(9)	0.132(8)
C21a	0.2678(9)	0.7383(7)	0.0810(10)	0.079(9)	F5	0.6123(8)	0.2024(6)	0.3004(10)	0.159(11)
C22a	0.3072(10)	0.7838(7)	0.1438(11)	0.088(10)	F6	0.5390(9)	0.2081(7)	0.4261(11)	0.197(13)
C23a	0.3557(8)	0.7579(6)	0.2219(10)	0.069(8)	O11	0.7501(6)	0.0014(5)	0.0617(8)	0.091(7)
C24a	0.3630(6)	0.6859(5)	0.2329(7)	0.048(6)	O12	0.6559(8)	0.0718(8)	−0.0302(8)	0.136(10)
C25a	0.2237(7)	0.4092(6)	−0.1023(8)	0.059(7)	O13	0.7104(7)	0.1214(6)	0.1187(12)	0.147(11)
C26a	0.2927(7)	0.4136(6)	−0.1757(8)	0.057(7)	O14	0.6435(7)	0.3192(5)	0.4458(8)	0.103(8)
C27a	0.3535(6)	0.4650(5)	−0.1331(7)	0.047(6)	O15	0.5952(12)	0.3490(9)	0.2855(11)	0.211(17)
C28a	0.4176(6)	0.4776(5)	−0.2117(7)	0.045(6)	O16	0.5059(9)	0.3614(8)	0.4200(14)	0.185(15)
C29a	0.5343(6)	0.5917(5)	0.2500(7)	0.047(6)	S3	0.0269(8)	0.5102(6)	0.7509(13)	0.429(18)
Mn3b	0.0984(1)	0.0588(1)	0.3162(1)	0.036(1)	O17	−0.0255(8)	0.5594(6)	0.7058(13)	0.140(6)
Mn4b	0.1635(1)	−0.0579(1)	0.3909(1)	0.037(1)	O18	0.1000(8)	0.5373(6)	0.7782(13)	0.148(7)
O1b	0.1447(4)	0.0364(3)	0.4316(4)	0.038(3)	O19	−0.0095(8)	0.4831(6)	0.8312(13)	0.300(22)
O2b	0.1250(4)	−0.0302(3)	0.268(5)	0.042(4)	C33	0.0452(12)	0.4432(10)	0.6724(13)	0.091(5)
O3b	−0.0076(4)	0.0439(3)	0.3531(4)	0.040(3)	F7	−0.0009(12)	0.4381(10)	0.5928(13)	0.118(4)
O4b	0.0394(4)	−0.0778(3)	0.4510(5)	0.046(4)	F8	0.0299(12)	0.3927(10)	0.7284(13)	0.211(10)
N1b	0.0626(5)	0.0926(4)	0.1759(5)	0.043(4)	F9	0.1209(12)	0.4312(10)	0.6429(13)	0.110(4)
N2b	0.0643(5)	0.1632(4)	0.3620(6)	0.042(4)	S4	0.2966(6)	0.1737(7)	0.6331(5)	0.264(10)
N3b	0.2036(5)	0.0954(4)	0.2696(6)	0.040(4)	O20	0.3293(6)	0.1070(7)	0.5977(5)	0.169(9)
N4b	0.2268(5)	−0.0967(4)	0.5215(6)	0.041(4)	O21	0.2425(6)	0.2035(7)	0.5649(5)	0.105(4)
N5b	0.2969(5)	−0.0531(4)	0.3593(6)	0.046(5)	O22	0.2618(6)	0.1733(7)	0.7274(5)	0.199(11)
N6b	0.1646(4)	−0.1646(4)	0.3529(6)	0.045(5)	C34	0.3661(10)	0.2161(9)	0.6164(14)	0.225(16)
C1b	0.0376(7)	0.1708(5)	0.1839(8)	0.053(6)	F10	0.4028(10)	0.1901(9)	0.5336(14)	0.146(6)
C2b	0.0283(6)	0.2001(5)	0.2918(8)	0.048(6)	F11	0.4202(10)	0.2167(9)	0.6883(14)	0.101(3)
C3b	−0.0125(7)	0.2664(6)	0.3171(10)	0.063(7)	F12	0.3403(10)	0.2816(9)	0.6040(14)	0.120(4)
C4b	−0.0131(9)	0.2929(7)	0.4137(11)	0.075(9)	OW1	0.1967(10)	0.1284(15)	0.8680(15)	0.154(13)
C5b	0.0275(8)	0.2551(6)	0.4856(10)	0.071(8)	OW2	0.0391(20)	0.1824(21)	0.9235(18)	0.550(46)

a) $U_{eq}=1/3(U_{11}+U_{22}+U_{33})$.

four lattice water molecules. All the non-hydrogen atoms of tetranuclear cations, two CF_3SO_3 anions, and two lattice water molecules were refined anisotropically, while for remaining two CF_3SO_3 anions only S atoms were refined anisotropically. Several cycles of refinement led to convergence with R=0.092 (R_w=0.117)). The high residual factor may be attributed to the low quality of the crystal. A final difference Fourier map showed the largest peak of 0.79 eÅ^{-3}. Final atomic coordinates for the non-hydrogen atoms are given in Table 2.[12] All calculations were carried out on a FACOM M760/20 computer at the Kanazawa University Information Processing Center.

Results and Discussion

Since tmdp contains two tripodal parts with N_3O donor set, the formation of di(μ-oxo)dimanganese core is expected. Oxygen donors such as alkoxide and phenolate have been shown to stabilize higher oxidation state of manganese ion. The presence of an alkoxo group makes manganese(II) ion easily air-oxidized to form a dimer-of-di(μ-oxo)manganese(III)manganese(IV)-dimers $[\{Mn_2(tmdp)(O)_2H_2O\}_2]^{4+}$. Hydrogen peroxide is also effective for oxidation of manganese(II) ion.

The electronic spectrum of **1** in acetonitrile showed absorption bands in the near infrared and visible regions at 13500 cm^{-1} (shoulder), 15920 cm^{-1} (ε=613 mol^{-1} cm^{-1} dm^3), 17090 cm^{-1} (shoulder), 18520 cm^{-1} (ε=553 mol^{-1} cm^{-1} dm^3), and 24390 cm^{-1} (shoulder), which resembles those for the di(μ-oxo)manganese(III)manganese(IV) complexes.[13] The complex is sufficiently stable in acetonitrile. The elctronic spectrum of **1** in solid state is essentially the same as that in acetonitrile, suggesting that the structure in solid state remains intact in acetonitrile.

Decription of the Structure of 1. The crystal structure consists of two crystallographically independent tetranuclear complex cations (molecule **a** and **b**[14]), CF_3SO_3 anions, and lattice waters. Each complex cation possesses an inversion center. Since the structures of two crystallographically unique tetranuclear cations are almost the same, only the molecular structure of **a** is given in Fig. 1. Selected bond distances and angles of the molecules **a** and **b** are given in Table 3. The complex cation consists of two di(μ-oxo)dimanganese dimers which are crystallographically equivalent and linked by two tmdp bridges to form a dimer-of-dimers with a bilayered structure having Mn1(**a** and **b**)···Mn2′(**a** and **b**) separations of 5.864(2) and 5.881(2) Å, respectively. Two Mn$<^{O}_{O}>$Mn planes are not faced directly, but slid as shown in Scheme 1. The Mn1(**a** and **b**)···Mn2(**a** and **b**) separations of 2.644(2) and 2.651(2) Å in dimers are almost at the lower end of the range (2.64—2.74 Å) for those of the di(μ-oxo)manganese(III)manganese(IV) complexes.[15] The bridging Mn–O(oxo)–Mn angles (93.5(3)—94.1(3)°) are also at the lower end of the range (94.0—97.7°) reported for other complexes.

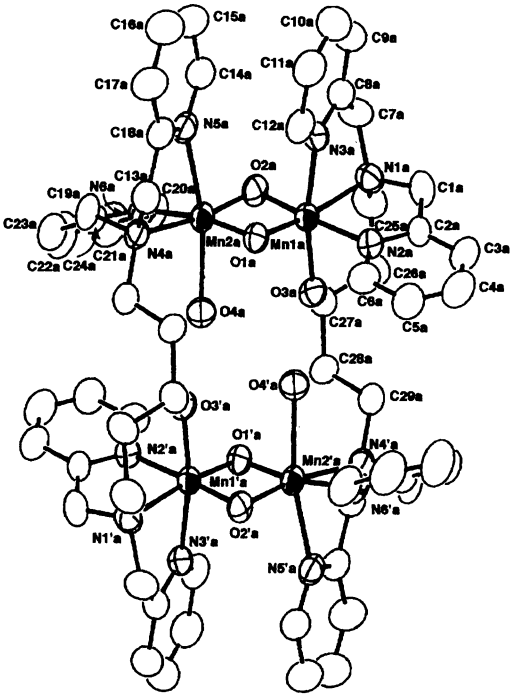

Fig. 1. View of the tetranuclear cation **1a** in **1** showing the atom numbering scheme.

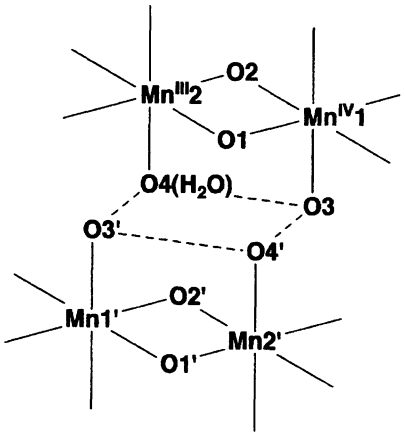

Scheme 1. A schematic drawing of hydrogen bonding network between di(μ-oxo)manganese(III)-manganese(IV) dimers.

These smaller angles are consistent with the shorter Mn1···Mn2 sparations. The manganese centers are in distorted octahedron with *cis,cis*-N_3O_3 donor set. The alkoxo groups (O3(**a** and **b**)) are bound axially only to Mn1(**a** and **b**). Although a similar structure has been found for $[(Mn_2O_2)_2(tphpn)_2]^{4+}$,[4j] two axially coordinated alkoxo groups serve as bridging ligands between Mn(III) and Mn(IV) ions of two di(μ-oxo)dimanganese cores. Such a bridging mode of alkoxo group is sterically difficult for the present complex. The average Mn1–O(oxo) bond of 1.784 Å is shorter than the Mn2–O(oxo) bond of 1.839 Å. The axial Mn1–O3(alkoxo) bonds of 1.876(6) and 1.878(6) Å are slightly shorter than the Mn–O(phenoxo) bond of 1.903(1) Å found for

Table 3. Selected Bond Lengths (l/Å) and Angles (ϕ/°) of **1**

Bond lengths				Bond angles			
Molecule **a**		Molecule **b**		Molecule **a**		Molecule **b**	
Mn1a–O1a	1.778(6)	Mn1b–O1b	1.781(6)	Mn1a–O1a–Mn2a	93.9(3)	Mn1b–O1b–Mn2b	94.1(3)
Mn1a–O2a	1.789(6)	Mn1b–O2b	1.789(6)	Mn1a–O2a–Mn2a	94.0(3)	Mn1b–O2b–Mn2b	93.5(3)
Mn1a–O3a	1.876(6)	Mn1b–O3b	1.878(6)	O1a–Mn1a–O2a	87.3(3)	O1b–Mn1b–O2b	87.7(3)
Mn1a–N1a	2.094(8)	Mn1b–N1b	2.094(7)	O1a–Mn1a–O3a	96.1(3)	O1b–Mn1b–O3b	95.7(3)
Mn1a–N2a	2.054(7)	Mn1b–N2b	2.070(7)	O1a–Mn1a–N1a	169.3(3)	O1b–Mn1b–N1b	170.2(3)
Mn1a–N3a	2.030(8)	Mn1b–N3b	2.052(8)	O1a–Mn1a–N2a	96.1(3)	O1b–Mn1b–N2b	96.2(3)
Mn2a–O1a	1.841(6)	Mn2b–O1b	1.841(6)	O1a–Mn1a–N3a	90.6(3)	O1b–Mn1b–N3b	91.3(3)
Mn2a–O2a	1.825(6)	Mn2b–O2b	1.849(6)	O2a–Mn1a–O3a	95.6(3)	O2b–Mn1b–O3b	95.4(3)
Mn2a–O4a	2.285(7)	Mn2b–O4b	2.286(7)	O2a–Mn1a–N1a	94.6(3)	O2b–Mn1b–N1b	93.9(3)
Mn2a–N4a	2.169(8)	Mn2b–N4b	2.174(8)	O2a–Mn1a–N2a	176.4(3)	O2b–Mn1b–N2b	176.1(3)
Mn2a–N5a	2.249(8)	Mn2b–N5b	2.264(8)	O2a–Mn1a–N3a	93.9(3)	O2b–Mn1b–N3b	94.4(3)
Mn2a–N6a	2.065(8)	Mn2b–N6b	2.061(8)	O3a–Mn1a–N1a	94.1(3)	O3b–Mn1b–N1b	93.8(3)
O3a–C27a	1.41(1)	O3b–C27b	1.43(1)	O3a–Mn1a–N2a	85.3(3)	O3b–Mn1b–N2b	84.4(3)
N1a–C1a	1.49(1)	N1b–C1b	1.51(1)	O3a–Mn1a–N3a	168.6(3)	O3b–Mn1b–N3b	168.1(3)
N1a–C7a	1.50(1)	N1b–C7b	1.51(1)	N1a–Mn1a–N2a	81.8(3)	N1b–Mn1b–N2b	82.3(3)
N1a–C25a	1.53(1)	N1b–C25b	1.51(1)	N1a–Mn1a–N3a	78.8(3)	N1b–Mn1b–N3b	78.9(3)
N2a–C2a	1.35(1)	N2b–C2b	1.32(1)	N2a–Mn1a–N3a	84.8(3)	N2b–Mn1b–N3b	85.4(3)
N2a–C6a	1.36(1)	N2b–C6b	1.35(1)	O1a–Mn2a–O2a	84.4(3)	O1b–Mn2b–O2b	84.1(3)
N3a–C8a	1.34(1)	N3b–C8b	1.34(1)	O1a–Mn2a–O4a	90.4(3)	O1b–Mn2b–O4b	90.0(2)
N3a–C12a	1.36(1)	N3b–C12b	1.35(1)	O1a–Mn2a–N4a	98.6(3)	O1b–Mn2b–N4b	100.5(3)
N4a–C13a	1.50(1)	N4b–C13b	1.49(1)	O1a–Mn2a–N5a	96.5(3)	O1b–Mn2b–N5b	95.0(3)
N4a–C19a	1.53(1)	N4b–C19b	1.52(1)	O1a–Mn2a–N6a	170.2(3)	O1b–Mn2b–N6b	170.4(3)
N4a–C29a	1.51(1)	N4b–C29b	1.51(1)	O2a–Mn2a–O4a	95.2(3)	O2b–Mn2b–O4b	95.5(3)
N5a–C14a	1.36(1)	N5b–C14b	1.36(1)	O2a–Mn2a–N4a	171.1(3)	O2b–Mn2b–N4b	170.6(3)
N5a–C18a	1.33(1)	N5b–C18b	1.33(1)	O2a–Mn2a–N5a	96.3(3)	O2b–Mn2b–N5b	96.8(3)
N6a–C20a	1.35(2)	N6b–C20b	1.35(1)	O2a–Mn2a–N6a	97.2(3)	O2b–Mn2b–N6b	95.8(3)
N6a–C24a	1.35(1)	N6b–C24b	1.33(1)	O4a–Mn2a–N4a	93.2(3)	O4b–Mn2b–N4b	92.7(3)
C1a–C2a	1.50(2)	C1b–C2b	1.52(1)	O4a–Mn2a–N5a	167.1(3)	O4b–Mn2b–N5b	167.1(3)
C2a–C3a	1.40(1)	C2b–C3b	1.40(1)	O4a–Mn2a–N6a	79.8(3)	O4b–Mn2b–N6b	80.4(3)
C3a–C4a	1.36(2)	C3b–C4b	1.35(2)	N4a–Mn2a–N5a	75.1(3)	N4b–Mn2b–N5b	74.8(3)
C4a–C5a	1.39(2)	C4b–C5b	1.38(2)	N4a–Mn2a–N6a	81.3(3)	N4b–Mn2b–N6b	81.0(3)
C5a–C6a	1.39(2)	C5b–C6b	1.41(2)	N5a–Mn2a–N6a	92.9(3)	N5b–Mn2b–N6b	94.5(3)
C7a–C8a	1.48(2)	C7b–C8b	1.51(1)	Mn1a–O3a–C27a	123.4(6)	Mn1b–O3b–C27b	124.9(5)
C8a–C9a	1.40(2)	C8b–C9b	1.39(2)	Mn1a–N1a–C1a	111.3(6)	Mn1b–N1b–C1b	110.5(5)
C9a–C10a	1.39(2)	C9b–C10b	1.40(2)	Mn1a–N1a–C7a	104.1(6)	Mn1b–N1b–C7b	105.2(6)
C10a–C11a	1.39(2)	C10b–C11b	1.38(2)	Mn1a–N1a–C25a	112.0(6)	Mn1b–N1b–C25b	112.2(6)
C11a–C12a	1.42(2)	C11b–C12b	1.40(2)	Mn1a–N2a–C2a	115.5(6)	Mn1b–N2b–C2b	114.9(6)
C13a–C18a	1.53(2)	C13b–C18b	1.51(2)	Mn1a–N2a–C6a	123.3(6)	Mn1b–N2b–C2b	122.4(6)
C14a–C15a	1.39(2)	C14b–C15b	1.39(2)	Mn1a–N3a–C8a	115.3(7)	Mn1b–N3b–C8b	115.6(6)
C15a–C16a	1.38(2)	C15b–C16b	1.40(2)	Mn1a–N3a–C12a	123.8(7)	Mn1b–N3b–C12b	124.4(6)
C16a–C17a	1.39(2)	C16b–C17b	1.38(2)	Mn2a–N4a–C13a	106.2(6)	Mn2b–N4b–C13b	107.5(6)
C17a–C18a	1.39(2)	C17b–C18b	1.40(2)	Mn2a–N4a–C19a	106.3(6)	Mn2b–N4b–C19b	107.2(6)
C19a–C24a	1.48(1)	C19b–C24b	1.52(1)	Mn2a–N4a–C29a	117.4(5)	Mn2b–N4b–C29b	116.2(5)
C20a–C21a	1.41(2)	C20b–C21b	1.37(2)	Mn2a–N5a–C14a	126.3(7)	Mn2b–N5b–C14b	125.8(7)
C21a–C22a	1.36(2)	C21b–C22b	1.39(2)	Mn2a–N5a–C18a	112.5(7)	Mn2b–N5b–C18b	113.6(6)
C22a–C23a	1.40(2)	C22b–C23b	1.40(2)	Mn2a–N6a–C20a	121.6(7)	Mn2b–N6b–C20b	122.4(7)
C23a–C24a	1.39(2)	C23b–C24b	1.39(2)	Mn2a–N6a–C24a	114.6(6)	Mn2b–N6b–C24b	116.6(6)
C25a–C26a	1.52(2)	C25b–C26b	1.53(1)				
C26a–C27a	1.54(2)	C26b–C27b	1.51(1)				
C27a–C28a	1.55(1)	C27b–C28b	1.54(1)				
C28a–C29a	1.54(1)	C28b–C29b	1.53(1)				
Mn1a–Mn2a	2.644(2)	Mn1b–Mn2b	2.651(2)				
Mn1a–Mn2′a	5.864(2)	Mn1b–Mn2′b	5.881(2)				

$[Mn^{IV}(salpn)O]_2$.[16] The axial Mn2–N5 bond distances (2.249(8)—2.264(8) Å) are significantly longer than the equatorial Mn2–N4 and Mn2–N6 bond distances (2.061(8)—2.174(8) Å). Such an elongation of the axial Mn2–N5 bonds is attributable to Jahn–Teller distortion of high-spin d^4 ion. The long axial Mn2–O4(coordinated water) bond distances (2.285(7) and 2.286(7) Å) are also subject to Jahn–Teller distortion. These results indicate that the oxidation states of Mn1 and Mn2 are four and three, respectively. The most striking feature

of the complex is that it has two water molecules coordinated to manganese(III) ions. The average O4–O4′ distance is 3.326 Å. This is the first example of a tetranuclear complex which contains two di(μ-oxo)manganese(III)manganese(IV) dimers and two coordinated water molecules in close proximity. Such coordinated water molecules must be of a key importance for modelling of OEC in PS II. The four oxygen atoms, O3, O4, O3′, and O4′, form a rhomboidal plane (see Scheme 1), where the average O3···O4 and O3···O4′ distances are 2.837 and 2.687 Å, respectively, and the angle of O3···O4···O3′ is 106°. These distances and angle suggest the presence of hydrogen bonding network between two alkoxo groups coordinated to Mn(IV) ions and two water molecules coordinated to Mn(III) ions.

Magnetic Susceptibility. The temperature dependence of the magnetic susceptibility of powdered sample of **1** was measured in the range 300—6 K (Fig. 2). The effective magnetic moment (Mn_4) decreases from 3.50 B.M. at 300 K to 2.50 B.M. at 80 K and is almost constant at 80—14 K. The values are smaller than the spin-only value (8.83 B.M. for an uncoupled $S=2\cdot S=3/2\cdot S=2\cdot S=3/2$ tetramer), indicating the presence of antiferromagnetic exchange interaction between manganese ions. Below 14 K, the effective magnetic moment increases slightly. The increment of the magnetic moment below 14 K is consistent with the observation of a "$\Delta M_s=2$" ESR signal at $g=4.5$ (vide infra).

There are two crystallographically independent tetranuclear species in solid state. Since the structures of the molecule **a** and **b** are almost identical as mentioned above, it is reasonable to assume that the magnetisms of these two species are the same. The magnetism for the present tetranuclear system is analyzed by the following isotropic exchange interaction model (1):

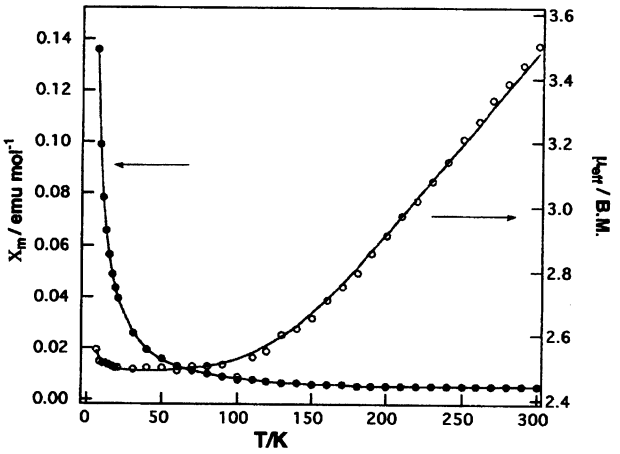

Fig. 2. Temperature dependences of the magnetic susceptibilites and the effective magnetic moments of **1**. The solid lines are the best fit curves with the parameters, $J_1=-145.4$ cm^{-1}, $J_2=-0.19$ cm^{-1}, $g=2.00$, and $TIP=3.35\times10^{-4}$ emu mol^{-1}.

$$\mathcal{H}=-2J_1\,(S_1\cdot S_2+S_3\cdot S_4)-2J_2\,(S_1\cdot S_4+S_2\cdot S_3)\,. \quad (1)$$

The exchange interaction scheme is defined in Scheme 2, where the interactions between S_1 and S_3, and between S_2 and S_4 are assumed to be neglected because they must be negligibly small compared to J_2. The eigen value-eigen vector equation given by $\mathcal{H}|\Phi_n(SM)>=E_n{}^{(0)}(S)|\Phi_n(SM)>$ has been solved numerically. In each spin manifold, the Zeeman interaction takes the form: $E_n{}^{(1)}(SM)H$, which reduces into $g\beta MH$ except for extreme low temperatures where the zero-field splitting can not be neglected. The magnetic susceptibility data were fitted to the Van–Vleck equation,

$$\chi=\frac{Ng^2\beta^2\sum_s(2S+1)S(S+1)\sum_n\exp\left(\frac{-E_n{}^{(0)}(S)}{kT}\right)}{3kT\sum_s(2S+1)\sum_n\exp\left(\frac{-E_n{}^{(0)}(S)}{kT}\right)}+TIP, \quad (2)$$

where TIP represents the temperature independent paramagnetism. All the energy levels that can significantly contribute to the magnetic susceptibility are listed in Table 4. It should be noted that these energy levels provide a corrected version of Kirk et al's.[6]

A good fit to the experimental data was obtained by $J_1=-145.4$ cm^{-1} and $J_2=-0.19$ cm^{-1}, $g=2.00$, and $TIP=3.35\times10^{-4}$ emu mol^{-1} (Fig. 2). The J_1 value is comparable to those of the di(μ-oxo)manganese(III)manganese(IV) complexes. The weak antiferromagnetic interaction (J_2) between S_1 and S_4, and S_2 and S_3 through the interdimer hydrogen bonding network with the interdimer distance of 5.9 Å (R_{D-D}) is consistent with the empirical J vs. R (distance between two metal ions) relationship established for a variety of dinuclear metal complexes linked by hydrogen bonding.[17] The antiferromagnetic exchange interaction within the di(μ-oxo)manganese(III)manganese(IV) dimer in $[(Mn_2O_2)_2(tphpn)_2]^{4+}$ ($J_1=-101$ cm^{-1})[6] is significantly smaller than that of **1**. As mentioned before, unlike the present complex, $[(Mn_2O_2)_2(tphpn)_2]^{4+}$ has two bridging alkoxo groups between the dimers which provide considerably larger antiferromagnetic

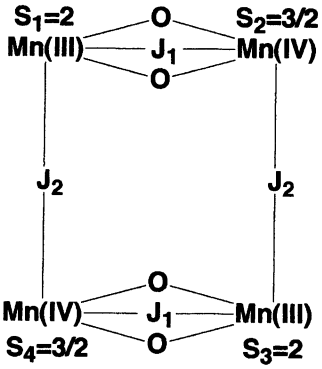

Scheme 2. Magnetic exchange interaction scheme of tetranuclear complex **1**.

Table 4. Energy Levels Which Significantly Contribute to the Magnetism of **1**

S	n	Energies
O	1	$18J_1-6J_2$
	2	$12J_1+2.4J_2$
1	1	$18J_1+2J_2$
	2	$15J_1+J_2$
	3	$15J_1-3J_2$
	4	$12J_1+1.76J_2$
	5	$7J_1+5.0J_2$
	6	$7J_1+3.88J_2$
2	1	$15J_1+6.6J_2$
	2	$15J_1-5.4J_2$
	3	$12J_1+0.48J_2$
	4	$10J_1+0.4J_2$
	5	$10J_1+0.4J_2$
	6	$7J_1+4.43J_2$
	7	$7J_1+1.07J_2$
3	1	$12J_1-1.44J_2$
	2	$10J_1-0.28J_2$
	3	$10J_1-0.29J_2$
	4	$7J_1+3.57J_2$
	5	$7J_1-3.15J_2$
4	1	$7J_1+2.43J_2$
	2	$7J_1-8.77J_2$

exchange interaction between the dimers ($J_2=-8.4$ cm^{-1}). The reduced antiferromagnetic interaction in the di(μ-oxo)manganese(III)manganese(IV) dimer in $[(Mn_2O_2)_2(tphpn)_2]^{4+}$ seems to be attributable to the structural and electronic perturbations arising from the bridging alkoxo groups. The energy separation between the triplet ground state and the first singlet excited state in **1** is ca. 1.52 cm^{-1}, which is still large enough to allow the use of spin hamiltonian for an isolated triplet state in order to interpret X-band ESR spectra.

ESR Spectra. Figure 3 shows a perpendicular-polarization X-band spectrum of powdered sample of **1** in acetonitrile at 13 K. The spectrum which consists of two broad signals centered around $g=2.0$ and $g=4.5$ can be reasonably interpreted as arising from the triplet ground state energetically well separated from the first excited state with non-zero spin. Those two signals correspond to the allowed "$\Delta M_s=1$" transition and the forbidden "$\Delta M_s=2$" transition, respectively (both of them obey the same selection rule: $\Delta M_s=\pm1$). Similar couples of such "$\Delta M_s=1$" and "$\Delta M_s=2$" signals have been observed in X-band ESR spectra of weak-antiferromagnetic exchange-coupled Cu(II)–Cu(II) dimers with an excited triplet state.[18]

A one-electron oxidized Mn_4(III,IV,IV,IV) species can be generated by constant potential electrolysis of **1** at 1.00 V vs. SCE in acetonitrile (vide infra). The oxidized species which consists of di(μ-oxo)manganese(III)manganese(IV) and di(μ-oxo)dimanganese(IV)

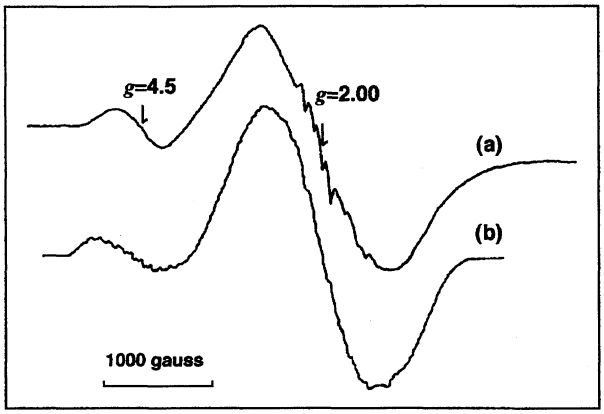

Fig. 3. ESR spectrum of powdered sample of **1** in acetonitrile at 13 K (a) and the simulated spectrum (b) with the parameters, $|D|=0.07$ cm^{-1}, $|E|=0.023$ cm^{-1}, $g=1.98$, $a_1=a_3=-90\times10^{-4}$ cm^{-1}, and $a_2=a_4=-85\times10^{-4}$ cm^{-1}.

species exhibits an ESR signal centered at $g=2.0$ with sixteen hyperfine lines due to ^{55}Mn nuclei (Fig. 4). The spectrum is characteristic of those of the di(μ-oxo)-manganese(III)manganese(IV) complexes. Thus, the ESR spectrum of di(μ-oxo)manganese(III)manganese(IV) unit is not affected by di(μ-oxo)dimanganese(IV) unit which is present in close proximity (probably ca. 5.9 Å apart from di(μ-oxo)manganese(III)manganese(IV)), suggesting that the di(μ-oxo)dimanganese(IV) unit is strongly antiferromagnetically coupled to yield an EPR silent species with $S=0$.

The "$\Delta M_s=2$" transition exactly vanishes when the static magnetic field (H) is directed along one of the principal molecular axes but has a finite transition probability when H is not parallel to any of them.[19] Its intensity and position in general depend upon zero-field splittings. A simple case of axial symmetry was theoretically investigated for the exchange-coupled Cu-

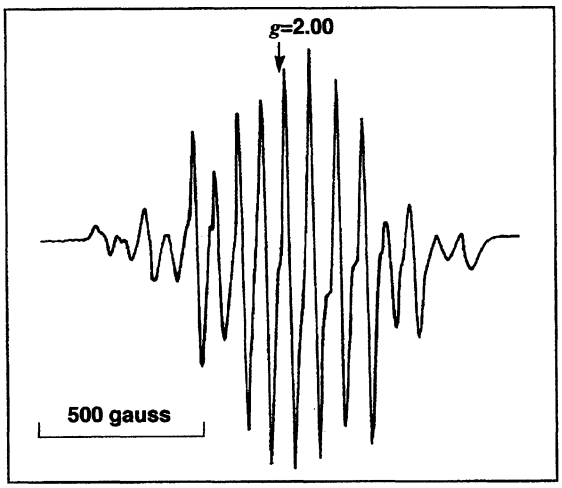

Fig. 4. ESR spectrum of powdered sample of the one-electron oxidized complex of **1** in acetonitrile at 77 K.

(II)–Cu(II) dimers.[20] In contrast, however, di(μ-oxo)-manganese(III)manganese(V) dimer $[Mn_2(bpy)_4(O)_2](ClO_4)_3 \cdot 3H_2O$ exhibited rather large zero-field splittings of near-rhombic symmetry in the first excited quartet state $|D_{12}| \cong 0.39$ cm^{-1} and $|E_{12}| = 0.12$ cm^{-1}.[21] This fact does not allow to assume axial symmetry for manganese tetramers with di(μ-oxo)manganese(III)-manganese(IV) unit. Furthermore, the effect of ^{55}Mn hyperfine interactions $\sum_i \boldsymbol{S}_i \cdot \boldsymbol{a}_i \cdot \boldsymbol{I}_i$ in the usual notations is essential in the observed line broadening. In order to simulate the ESR spectra, however, we assume for simplicity that all the monomeric $\boldsymbol{g}_i$- and $\boldsymbol{a}_i$-tensors (i=1—4) are isotropic, and solve the eigen vector-eigen value problem of the spin hamiltonian (3) for a general direction of $\boldsymbol{H}$ with respect to the molecular coordinate system:

$$\mathscr{H} = \beta g \boldsymbol{S} \cdot \boldsymbol{H} + \sum_{i=1}^{4} P_i a_i \boldsymbol{S} \cdot \boldsymbol{I}_i + \boldsymbol{D}\left(S_z^2 - 2/3\right) + \boldsymbol{E}\left(S_x^2 - S_y^2\right), \quad (3)$$

where $g = \sum_{i=1}^{4} P_i g_i$, $P_i = < \Phi_0(SM)|S_i \cdot S|\Phi_0(SM) > /[S(S+1)]$, which is called "projection factors",[22] and the spin wave function in the triplet ground state $|\Phi_0(SM)>$ is given by $|S_{12}(1/2)S_{34}(1/2)S(1)M>$ in the zeroth approximation of J_2, where $\boldsymbol{S}_{12} = |\boldsymbol{S}_{12}| = |\boldsymbol{S}_1 + \boldsymbol{S}_2|$ and $\boldsymbol{S}_{34} = |\boldsymbol{S}_{34}| = |\boldsymbol{S}_3 + \boldsymbol{S}_4|$. Then, P_i (i=1—4) are readily found to be 1 for Mn(III) ions and −0.5 for Mn(IV) ions. Various computer simulations were performed using a program written by Kusunoki which performs the iterative diagonalization of $\mathscr{H}$ over a large number of magnetic field directions. The simulations involve proper computations of the transition matrix element of the Zeeman interactions as well as the magnetization denominator. It took ca. 2 h per each simulation by use of Fujitsu VP2200/10 computer in Meiji University. As shown in Fig. 3, an excellent fit was obtained for a reasonable set of parameters: $|D| = 0.07$ cm^{-1}, $|E| = 0.023$ cm^{-1}, $g = 1.98$, $a_1 = a_3 = -90 \times 10^{-4}$ cm^{-1} and $a_2 = a_4 = -85 \times 10^{-4}$ cm^{-1}.

The origins of zero-field splittings which have been examined so far involve the single ion crystal field effect, the dipole–dipole interaction and the pseudo-dipolar (or anisotropic exchange) interaction due to a single ion spin-orbit coupling. In general, the zero-field splittings in a spin system can take place only when the spin is not less than 1. Therefore, if both the di(μ-oxo)manganese-(III)manganese(IV) dimers in the tetramer have rigid spins of $S_{12} = S_1 - S_2 = 1/2$ and $S_{34} = S_3 - S_4 = 1/2$ (see Scheme 2), the zero-field splitting tensors, $\boldsymbol{D}_{III}$, $\boldsymbol{D}_{IV}$, and $\boldsymbol{D}_{III\cdot IV}$, due to Mn(III), Mn(IV) and a pair of Mn-(III)-Mn(IV) ions in each dimer, respectively, can not contribute to the total zero-field splitting described by tensor $\boldsymbol{D}$. Then the interdimer dipole–dipole interaction and the interdimer pseudo-dipolar interaction alone would be origins of $\boldsymbol{D}$. The former takes the form:[23]

$$\boldsymbol{D}_{dip} = 2\boldsymbol{D}_{13} - \boldsymbol{D}_{14} - \boldsymbol{D}_{23} + 0.5\boldsymbol{D}_{24};$$
$$\boldsymbol{D}_{ij} = \left(\beta^2 g_i g_j / r_{ij}^3\right)[\boldsymbol{I} - 2\hat{\boldsymbol{r}}_{ij}\hat{\boldsymbol{r}}_{ij}],$$

where $\boldsymbol{I}$ is a unit tensor, and $\hat{\boldsymbol{r}}_{ij} = \boldsymbol{r}_{ij}/r_{ij}$. For a rectangular Mn_4(III,IV,III,IV)tetramer with equivalent Mn-(III)–Mn(IV) distances of 2.65 Å in two di(μ-oxo)-manganese(III)manganese(IV) units, zero-field splitting parameters, D_{dip} and E_{dip}, arising from the interdimer dipole–dipole interaction were evaluated as function of the interdimer distance (R_{D-D}), as depicted in Fig. 5, in which the principal y'-axis was taken normal to the plane and then the principal z'-axis was found to be from 3.27° to 7.33° inclined to the S_1–S_4 (S_2–S_3) direction (see Scheme 2) as R_{D-D} increases from 2.5 to 6.5 Å. Contrary to a simple-minded estimation in reference 6, D_{dip} is always positive and takes the values 0.098 cm^{-1} at $R_{D-D} = 3.96$ Å for $[(Mn_2O_2)_2(tphpn)_2]^{4+}$ and 0.021 cm^{-1} at $R_{D-D} = 5.9$ for **1**. The rhombic component E_{dip} is also positive and negligibly small. Thus, it is concluded that the interdimer dipole–dipole interaction may be neglected for the present tetramer with $R_{D-D} = 5.9$ Å, and also for $[(Mn_2O_2)_2(tphpn)_2]^{4+}$ ($D = 1.8$ cm^{-1}) with $R_{D-D} = 3.96$ Å.

Kirk et al. suggested that the interdimer pseudo–dipolar interaction (D_{aex}) is a principal origin for the zero-field splittings in $[(Mn_2O_2)_2(tphpn)_2]^{4+}$.[6] According to the common knowledge, however, this interaction must be of the order $|\boldsymbol{D}_{aex}| \cong 2|J_2^*(2-g)^2|$, where J_2^* is the effective exchange integral between the excited-state orbitals of Mn1(IV) and Mn2′(III) ions (Fig. 1). For $[(Mn_2O_2)_2(tphpn)_2]^{4+}$ ($J_2 = -8.4$ cm^{-1} and $g = 2.01$), D_{aex} is estimated to be at most 0.02 cm^{-1}, assuming that J_2^* is ten times larger than J_2. Similarly, for the present complex ($J_2 = -0.19$ cm^{-1} and $g = 1.98$), D_{aex} is negligibly small compared with the observed $|D|$ (0.07 cm^{-1}). Therefore, the observed zero-field splittings for

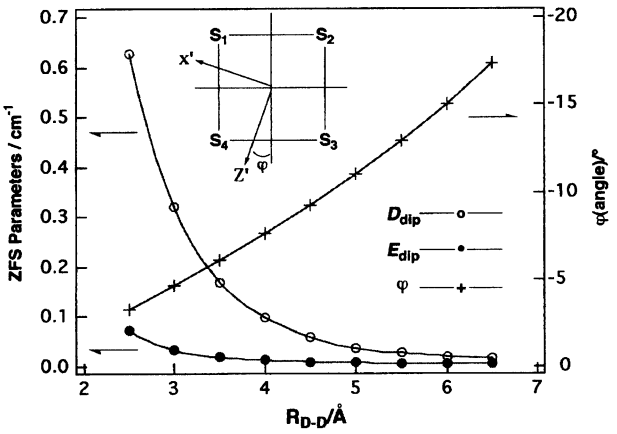

Fig. 5. Dependence of the magnetic dipolar coupling parameters D_{dip} (○) and E_{dip} (●), and φ defined in the Figure on the interdimer distance R_{D-D}, where Mn(III)–Mn(IV) distances within two di(μ-oxo)manganese(III)manganese(IV) dimers are 2.65 Å. The principal axes of tensor $\boldsymbol{D}_{dip}$ are also depicted.

these compounds must arise from the other effects than dipole–dipole and pseudo-dipolar interactions between two dimers. Namely, the pre-assumption of rigid composite spins must be relaxed by allowing a partial population in the higher $S_{12}=3/2$ and $S_{34}=3/2$ spin excited states.

In the second order pertubation theory with respect to J_2, the ground state wave function $|\Phi_0(SM)>$ changes into

$$\begin{aligned}|\Phi_0(SM)\rangle \cong & |S_{12}(1/2)S_{34}(1/2)S(1)M\rangle \\ & - \{2J_2/(J_1+J_2)\} \\ & \times \{|S_{12}(3/2)S_{34}(1/2)S(1)M\rangle \\ & + |S_{12}(1/2)S_{34}(3/2)S(1)M\rangle\} \end{aligned} \quad (4)$$

where we used the matrix elements, $<3/2,1/2,1,M|S_1\cdot S_4|1/2,1/2,1,M>=<1/2,3/2,1,M|S_2\cdot S_3|1/2,1/2,1,M>=1$, and $<3/2,1/2,1,M|S_2\cdot S_3|1/2,1/2,1,M>=<1/2,3/2,1,M|S_1\cdot S_4|1/2,1/2,1,M>=2$, etc.[24] To proceed further, one needs to calculate some non-diagonal matrix elements of the second rank tensor operators. This theoretical work will be published elsewhere.[23] Here, we use only the result (Eq. 5):

$$\begin{aligned}\boldsymbol{D} \cong & \{J_2/(J_1+J_2)\}(16.8\boldsymbol{D}_{\mathrm{III}}+4.8\boldsymbol{D}_{\mathrm{IV}}-10.8\boldsymbol{D}_{\mathrm{III-IV}}) \\ & +\boldsymbol{D}_{\mathrm{dip}}+\boldsymbol{D}_{\mathrm{aex}}, \end{aligned} \quad (5)$$

where $\boldsymbol{D}_{\mathrm{III}}$, $\boldsymbol{D}_{\mathrm{IV}}$, and $\boldsymbol{D}_{\mathrm{III-IV}}$ are symmetric traceless tensors for manganese(III), manganese(IV) and di(μ-oxo)manganese(III)manganese(IV) spins, respectively. Usually, the zero-field splitting constants of d^4 ions are much larger than those of d^3 ions because of the Jahn–Teller distortion of the crystal field.[25] The $|D_{\mathrm{III}}|$ and $|E_{\mathrm{III}}|$ values of Mn(III) ions in TiO_2 amount to 3.4 and 1.2 cm^{-1}, respectively.[21,25] The $\boldsymbol{D}_{\mathrm{III-IV}}$ tensor in general includes both the effects of dipole–dipole and pseudo-dipolar interactions within the dimer, but the latter contribution is estimated to be negligibly small (less than 0.01 cm^{-1})[21] compared with the former, resulting in the axial zero-field splitting constants: $D_{\mathrm{III-IV}}\cong -3g^2\beta^2/r^3\cong -0.27$ cm^{-1} for $g=2$ and $r=2.65$ Å (Mn(III)–Mn(IV) distance in di(μ-oxo)-manganese(III)manganese(IV) dimer) with $|E_{\mathrm{III-IV}}|\ll 0.01$ cm^{-1}.[21] Hence, the dominant contribution in Eq. 5 must arise from the crystal field effect of the two Mn(III) ions. The only reported example (Mn(III) in TiO_2) mentioned above nearly satisfies the rhombic symmetry ($|D_{\mathrm{III}}|/|E_{\mathrm{III}}|\cong 2.8$) which is in good agreement with the observation in our system ($|D|/|E|\cong 3.0$). Furthermore, the present theory reasonably explains why such large zero-field splittings are observed in the tetrameric dimer-of-dimers, **1** and $[(Mn_2O_2)_2(tphpn)_2]^{4+}$.[6] The values D_{III} and E_{III} are expected to somewhat depend upon the surrounding ligands of Mn(III) ions. In fact, the D_{III} values are reported to fall in the range of -1 to -4 cm^{-1}.[26,27] Hence, it is better to inversely determine D_{III} and E_{III} from the observed D and E values. With use of $J_1=-145$ cm^{-1} and $J_2=-0.19$ cm^{-1}, obtained from the temperature dependence of the magnetic susceptibility, and $|D|=0.07$ cm^{-1} and $|E|=0.023$ cm^{-1}, we get $|D_{\mathrm{III}}|=3.2$ cm^{-1} and $|E_{\mathrm{III}}|=1.0$ cm^{-1} which are in good agreement with the typical values of Mn(III) ions: $|D_{\mathrm{III}}|=3.4$ cm^{-1} and $|E_{\mathrm{III}}|=1.2$ cm^{-1} in TiO_2,[21,25] $D_{\mathrm{III}}=-1$——-4 cm^{-1} in Mn(III) Schiff-base complexes,[26] and $D_{\mathrm{III}}=-1$——-2.3 cm^{-1} in Mn(III) porphyrin complexes.[27] In conclusion, the main origin of the zero-field splittings in the tetrameric dimer-of-di(μ-oxo)manganese(III)manganese(IV)-dimers is not the interdimer pseudo–dipolar interaction as was assumed by Kirk et al.[6] but the crystal-field effect due to two Mn(III) ions that is caused by a mixing of excited-state spin configurations into the triplet ground state via the isotropic interdimer exchange interactions (J_2). The fact that the crystal field associated with D_{III} is not axial but rhombic may reflect the presence of di(μ-oxo) bridge.

Electrochemistry. Cyclic voltammogram (CV) of **1** in acetonitrile at 20 °C is shown in Fig. 6. Complex **1** exhibits a quasi-reversible wave at 0.96 V vs. SCE. Constant potential coulommetry at 1.00 V vs. SCE revealed that the redox couple corresponds to a one-electron transfer (0.95 electron: Mn_4(III, IV, IV, IV)/Mn_4 (III, IV, III, IV) couple). The formation of Mn_4(III, IV, IV, IV) species is confirmed by ESR measurement as described above. This one-electron transfer indicates that two Mn(III) moieties in a tetranuclear unit are electrochemically inequivalent and some interaction is present between the dimers separated by ca. 5.9 Å so that oxidation of only one of two Mn(III) moieties in two dimers occurs. Electrostatic interaction and/or hydrogen bonding network between coordinated water molecules and axial alkoxo groups seem to be responsible for this single oxidation of the dimers. $E_{1/2}$(IV/III) value of Mn(III) moiety containing a coordinated water molecule is comparable to those of the tpa,[13b] bispicen and related complexes[13c] with N_4O_2 donor set (0.98—1.04 V vs. SCE) and higher than that of the N_3O-py

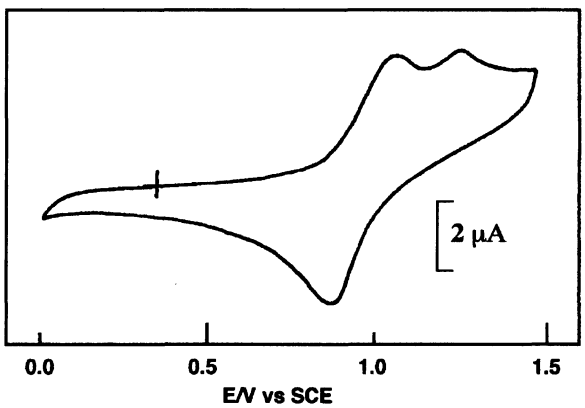

Fig. 6. Cyclic voltammogram of **1** in acetonitrile containing 0.1 M $[N(n\text{-}Bu)_4]ClO_4$ at a glassy carbon electrode with a scan rate 100 $mV\,s^{-1}$.

complex[28] (0.78 V vs. SCE) which has N_3O_3 donor set with a coordinated carboxylato group. Although in order to investigate the deprotonation behavior of the coordinated water molecules, we tried to measure CV at various pH's in acetate and phosphate buffers, it was found that some decomposition of the complex occured in these buffer solutions. An irreversible oxidation wave is observed at 1.20 V vs. SCE. It was expected that the complex serves as a two-electron oxidant with such high oxidation potentials. In order to generate an Mn_4(IV, IV, IV, IV) species, constant potential electrolysis was carried out at 1.25 V vs. SCE. However, insoluble material which seems to be MnO_2 was deposited on an electrode and only 0.5—0.6 electron transfer/Mn_4 was observed. The result implies that Mn_4(IV, IV, IV, IV) species is unstable toward hydrolysis to give insoluble MnO_2.

We wish to thank Professor Takesi Sakurai of Kanazawa University for allowing us to use the ESR spectrometer. The present study was supported by a Grant-in-Aid for Scientific Research on Priority Areas No. 03241105 by the Ministry of Education, Science and Culture to which our thanks are due.

References

1) K. Sauer, *Acc. Chem. Res.*, **13**, 249 (1980); G. S. Dismukes, *Photochem. Photobiol.*, **43**, 99 (1986); G. Renger, *Angew. Chem., Int. Ed. Engl.*, **26**, 643 (1987); G. Christou, *Acc. Chem. Res.*, **22**, 328 (1989); K. Wieghardt, *Angew. Chem., Int. Ed. Engl.*, **28**, 1153 (1989); G. W. Brudvig and R. H. Crabtree, *Prog. Inorg. Chem.*, **37**, 99 (1989).

2) B. Kok, B. Forbush, and M. McGloin, *Photochem. Photobiol.*, **11**, 457 (1970).

3) G. C. Dismukes, K. Ferris, and P. Watnick, *Photochem. Photobiol. Phys.*, **3**, 243 (1982); J. C. de Paula, W. F. Beck, and G. W. Brudvig, *J. Am. Chem. Soc.*, **108**, 4002 (1986); V. K. Yachandra, R. D. Guiles, A. E. Mcdermott, J. L. Cole, R. D. Britt, S. L. Dexheimer, K. Sauer, and M. P. Klein, *Biochemistry*, **26**, 5974 (1987); M. Kusunoki, T. Ono, T. Matsushita, H. Oyanagi, and Y. Inoue, *J. Biochem.*, **29**, 407 (1990).

4) a) K. Wieghardt, U. Bossek, and W. Gebert, *Angew. Chem., Int. Ed. Engl.*, **22**, 328 (1983); b) J. S. Bashkin, H. R. Chang, W. E. Streib, J. C. Huffman, D. N. Hendrickson, and G. Christou, *J. Am. Chem. Soc.*, **109**, 6502 (1987); c) K. Wieghardt, U. Bossek, B. Nuber, J. Weiss, J. Bonvoisin, M. Corbella, S. E. Vitols, and J. J. Girerd, *J. Am. Chem. Soc.*, **110**, 7398 (1988); d) K. S. Hagen, T. D. Westmoreland, M. J. Scott, and W. H. Armstrong, *J. Am. Chem. Soc.*, **111**, 1907 (1989); e) J. B. Vincent, C. Christmas, H. R. Chang, Q. Li, P. D. W. Boyd, J. C. Huffman, D. N. Hendrickson, and G. Christou, *J. Am. Chem. Soc.*, **111**, 2086 (1989); f) M. Suzuki, T. Sugisawa, H. Senda, H. Oshio, and A. Uehara, *Chem. Lett.*, **1989**, 1091; g) M. K. Chan and W. H. Armstrong, *J. Am, Chem. Soc.*, **111**, 9121 (1989); h) M. Suzuki, H. Senda, M. Suenaga, T. Sugisawa, and A. Uehara, *Chem. Lett.*, **1990**, 923; i) M. K. Chan and W. H. Armstrong, *J. Am. Chem. Soc.*, **112**, 4985 (1990); j) M. K. Chan and W. H. Armstrong, *J. Am. Chem. Soc.*, **113**, 5055 (1991); k) M. Mikuriya, Y. Yamato, and T. Tokii, *Chem. Lett.*, **1991**, 1429.

5) S. L. Dexheimer and M. P. Klein, *J. Am. Chem. Soc.*, **114**, 2821 (1992).

6) M. L. Kirk, M. K. Chan, W. H. Armstrong, and E. I. Solomon, *J. Am. Chem. Soc.*, **114**, 10432 (1992).

7) M. Suzuki, T. Sugisawa, and A. Uehara, *Bull. Chem. Soc. Jpn.*, **63**, 1115 (1990).

8) F. E. Mabbs and D. J. Marchin, "Magnetisms and Transition Metal Complexes," Chapman and Hall, London (1975), p. 5.

9) G. M. Sheldrick, "SHELXS-86. A Program for Crystal Structure Determination," University of Göttingen, FRG (1986).

10) G. M. Sheldrick, "SHELX-76. A Program for Crystal Structure Determination," Cambridge University, Cambridges, UK (1976).

11) "International Tables for X-Ray Crystallography," Kynoch Press, Birmingham, England (1974), Vol. IV.

12) Table of thermal parameters including anisotropic thermal parameters and $F_o - F_c$ table are deposited as Document No. 67031 at the Office of the Editor of Bull. Chem. Soc. Jpn.

13) a) S. R. Cooper and M. Calvin, *J. Am. Chem. Soc.*, **100**, 7248; b) M. Suzuki, H. Senda, M. Suenaga, T. Sugisawa, and A. Uehara, *Chem. Lett.*, **1988**, 477; c) P. A. Goodson, J. Glerup, D. J. Hodgson, K. Michelsen, and E. Pedersen, *Inorg. Chem.*, **29**, 503 (1990).

14) The atom numbering scheme of the molecule **b** corresponds to that of the molecule **a** shown in Fig. 1.

15) P. A. Goodson and D. J. Hodgson, *Inorg. Chim. Acta*, **172**, 49 (1990); A. R. Oki J. Glerup, and D. J. Hodgson, *Inorg. Chem.*, **29**, 2435 (1990), and references therein.

16) J. W. Gohdes and W. H. Armstrong, *Inorg. Chem.*, **31**, 368 (1992).

17) a) R. E. Coffman and G. R. Buettner, *J. Phys. Chem.*, **83**, 2392 (1979); b) M. Ardon, A. Bino, K. Michelsen, and E. Pedersen, *J. Am. Chem. Soc.*, **109**, 5855 (1987), and references therein.

18) T. R. Felthouse and D. N. Hendrickson, *Inorg. Chem.*, **17**, 444 (1978).

19) S. P. McGlynn, T. Asumi, and M. Kinoshita, "Molecular Spectroscopy of the Triplet State," Prentice-Hall, Inc., Englewood Cliffs, New Jersey (1969), pp. 353—357.

20) J. H. Price, J. R. Pilbrow, K. S. Murray, and T. D. Smith, *J. Chem. Soc. A*, **1970**, 968.

21) M. Inoue, *Bull. Chem. Soc. Jpn.*, **51**, 1400 (1978).

22) M. Kusunoki, *Chem. Phys. Lett.*, **197**, 108 (1992).

23) K. Hasegawa and M. Kusunoki, Manuscript in preparation.

24) J. S. Griffith, *Mol. Phys.*, **24**, 833 (1972).

25) A. Abragam and B. Bleaney, "Electron Paramagnetic Resonance of Transition Ions," Clarendon Press, Oxford (1970).

26) B.J. Kennedy and K. S. Murray, *Inorg. Chem.*, **24**, 1552 (1985).

27) B. J. Kennedy and K.S. Murray, *Inorg. Chem.*, **24**, 1557 (1985).

28) M.Suzuki, J. Senda, Y. Kobayashi, H. Oshio, and A. Uehara, *Chem. Lett.*, **1988**, 1763.